JACS
JOURNAL OF THE AMERICAN CHEMICAL SOCIETY

ARTICLE

pubs.acs.org/JACS

Imaging Protein−Protein Interactions inside Living Cells via Interaction-Dependent Fluorophore Ligation

Sarah A. Slavoff,[‡] Daniel S. Liu, Justin D. Cohen, and Alice Y. Ting*

Department of Chemistry, Massachusetts Institute of Technology, Cambridge, Massachusetts

Supporting Information

ABSTRACT: We report a new method, Interaction-Dependent PRobe Incorporation Mediated by Enzymes, or ID-PRIME, for imaging protein−protein interactions (PPIs) inside living cells. ID-PRIME utilizes a mutant of *Escherichia coli* lipoic acid ligase, LplA^{W37V}, which can catalyze the covalent ligation of a coumarin fluorophore onto a peptide recognition sequence called LAP1. The affinity between the ligase and LAP1 is tuned such that, when each is fused to a protein partner of interest, LplA^{W37V} labels LAP1 with coumarin only when the protein partners to which they are fused bring them together. Coumarin labeling in the absence of such interaction is low or undetectable. Characterization of ID-PRIME in living mammalian cells shows that multiple protein−protein interactions can be imaged (FRB−FKBP, Fos−Jun, and neuroligin−PSD-95), with as little as 10 min of coumarin treatment. The signal intensity and detection sensitivity are similar to those of the widely used fluorescent protein complementation technique (BiFC) for PPI detection, without the disadvantage of irreversible complex trapping. ID-PRIME provides a powerful and complementary approach to existing methods for visualization of PPIs in living cells with spatial and temporal resolution.

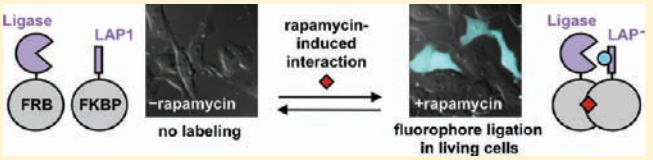

INTRODUCTION

The functions of proteins in the complex intracellular environment are governed by their interactions with other proteins. Classical biochemical methods to investigate protein−protein interactions (PPIs), such as co-immunoprecipitation, rely on cell lysis, which can result in both false positives and false negatives due to dilution, mixing, washing, and non-specific binding. Therefore, methods to interrogate PPIs in their native context, the living cell, are advantageous. Bimolecular fluorescence complementation (BiFC), based on fluorescent protein reconstitution, and other protein complementation assays (PCAs) have been applied to visualize hundreds of PPIs in living cells. However, BiFC has several limitations. First, the time for fluorophore maturation after reconstitution is >1 h, limiting the temporal resolution.[1] Second, the formation of a fluorescent protein from its fragments is irreversible,[2] trapping the interacting proteins in a complex, potentially disrupting trafficking, preventing turnover, or prolonging signaling. Third, BiFC can give false positive signals due to the high affinity of the reporter fragments for each other.[3−5] New and complementary methods are therefore needed.

We previously reported an enzymatic indicator of PPIs based on proximity-dependent biotinylation.[6] In this scheme, the enzyme biotin ligase (BirA) and a substrate acceptor peptide, called the AP(-3) (which consists of the originally reported BirA acceptor peptide (AP),[7,8] truncated by three amino acids from the C terminus), are fused to interacting proteins. BirA has a high K_m for the AP(-3), such that only when an interaction occurs can BirA catalyze biotin attachment to the AP(-3); detecting the ligated biotin with streptavidin reports on the interaction. This method was applied to the visualization of the rapamycin-dependent interaction of FRB (the FKBP−rapamycin-binding domain of the mammalian target of rapamycin and FKBP (or FK506 binding protein) as well as the interaction of the cell-cycle regulator Cdc25c with 14-3-3ε, a protein that binds phosphorylated interaction partners. Proximity-dependent biotinylation has some advantages over BiFC. While the labeling is covalent, complexes are not trapped; total labeling time is significantly shorter; and false positives are reduced due to low affinity between BirA and its peptide substrate AP(-3). However, due to the requirement for streptavidin staining to detect biotinylation, this method is limited to PPI imaging on the surface of living cells, or inside cells after the cells are fixed and permeabilized.[6] Here we extend the methodology with the development of a new enzymatic ligation PPI reporter that works in one step, inside living cells, with a single small-molecule fluorescent label.

The reporter is based on the *Escherichia coli* enzyme lipoic acid ligase (LplA), which we have previously engineered to site-specifically incorporate various probes and functional group handles onto peptide substrates, including alkyl azides and alkynes,[9] an aryl azide photocross-linker,[10] and a coumarin fluorophore.[11] Specifically, we make use of the mutant LplA^{W37V}, which covalently ligates the blue fluorophore coumarin to a specific lysine residue of the LplA acceptor peptide (LAP).[11] We engineer this system to create a low-background, live-cell PPI-labeling method we call Interaction-Dependent PRobe Incorporation Mediated by Enzymes (ID-PRIME). We apply ID-PRIME to imaging of the rapamycin-dependent interaction of FRB and FKBP, the heterodimerization of the leucine zipper domains of Fos and Jun, and the interaction of the neuronal proteins PSD-95 and neuroligin-1.

Received: July 11, 2011
Published: November 18, 2011

A

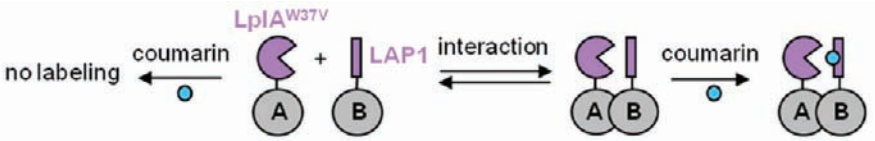

B

Enzyme	Peptide	Probe	K_m for Peptide	k_{cat}	Reference
BirA	AP	biotin	25 μM	12 min^{-1}	[7]
BirA	AP(-3)	biotin	345 μM	0.53 min^{-1}	[6]
LplA	LAP2	lipoic acid	13 μM	13.2 min^{-1}	[12]
$LplA^{W37V}$	LAP2	coumarin	not determined†	1.14 min^{-1}	[11]
LplA	LAP1	8-azido-octanoic acid	>300 μM	2.88 min^{-1}	[9]
$LplA^{W37V}$	LAP1	coumarin	>500 μM	>0.45 min^{-1}	this work

Figure 1. Scheme for interaction-dependent PRIME (ID-PRIME) for protein−protein interaction detection, and kinetic parameters. (A) Interaction between proteins A and B promotes covalent fluorophore ligation to the fused peptide (LAP1), catalyzed by the fused ligase enzyme ($LplA^{W37V}$). In the absence of an interaction, no ligation occurs. (B) Summary of kinetic parameters from previous studies and this work. Rate constants relevant to *Escherichia coli* biotin ligase (BirA) are shaded red.[6,7] Rate constants relevant to LplA are shaded blue.[9,11,12] AP is BirA′s 15-amino acid acceptor peptide. AP(-3) is a truncated AP with three amino acids removed from the C terminus.[6] The low-affinity LAP sequence (LAP1) used for ID-PRIME is DEVLVEIETDKAVLEVP.[9] The high-affinity LAP sequence (LAP2) used for conventional, non-interaction-dependent PRIME labeling is GFEIDKVWYDLDA.[12] The lysine site labeled by the enzyme is underlined. † While the K_m of LplA for LAP2 has not been determined in the presence of coumarin substrate, this value is expected to be similar to the 13 μM value observed in the presence of lipoic acid.

RESULTS AND DISCUSSION

Figure 1A illustrates the concept of ID-PRIME. In this scheme, A and B are two interacting proteins. LplA is fused to protein A, and LplA′s peptide substrate, LAP, is fused to protein B. If A and B do not interact, the enzyme and peptide do not associate, and no labeling occurs.

The system is engineered to provide high labeling sensitivity when an interaction occurs and low background in the absence of an interaction. We do so by treating the interaction as a kinetic switch; when no interaction occurs, the rate of LAP labeling by LplA is undetectably slow and, when an interaction does occur, the labeling rate is maximally fast. Such switching depends on the kinetic parameters. In the absence of a PPI, if the protein concentrations in the cell are far below the LplA−LAP K_m, the bimolecular reaction rate will be governed by k_{cat}/K_m. In the presence of a PPI, on the other hand, when the local concentration of LAP with respect to LplA is very high, the pseudo-zero-order reaction rate will be governed by k_{cat}. Therefore, by engineering high K_m, we minimize background labeling, and by engineering high k_{cat}, we maximize signal in the presence of a PPI.

The kinetic parameters of both BirA and LplA ligases are shown in Figure 1B. In order to make BirA-mediated biotinylation interaction-dependent, we previously designed a modified acceptor peptide, the AP(-3), that had a high K_m of 345 μM compared to 25 μM for the original, full-length AP.[6] We reasoned that interaction-dependent labeling could also be accomplished with LplA. In particular, our first-generation rationally designed peptide substrate, which we refer to as LAP1, has a high K_m (>300 μM),[9] in contrast to the second-generation LAP2 sequence that is currently used for PRIME applications (K_m 13 μM).[12] Despite LAP1's higher K_m, we previously found that the k_{cat} for LplA-catalyzed ligation of an alkyl azide probe onto LAP1 (2.88 ± 0.06 min^{-1}) was only about 2-fold slower than for ligation to the natural protein substrate of LplA, E2p.[9] It therefore seemed that LAP1 possessed the right combination of high K_m and high k_{cat} for interaction-dependent labeling.

Interaction-Dependent Lipoic Acid Ligation in vitro and in Cells. In order to determine the suitability of the LplA−LAP1 pair for detecting PPIs, we first investigated interaction-dependent labeling with LplA's natural small-molecule substrate, lipoic acid. We utilized the rapamycin-dependent interaction of FRB and FKBP proteins as our model system, fusing LplA to the C terminus of FRB and LAP1 to the C terminus of FKBP, since the crystal structure of the FRB−rapamycin−FKBP complex indicates that these ends are only 18 Å apart (Figure 2A).[13]

We found that interaction-dependent lipoylation of FKBP-LAP1 by FRB-LplA could be detected in vitro using purified proteins combined at 10 μM each with a +/− rapamycin signal-to-background ratio of >12:1 by anti-lipoic acid immunoblot analysis (Figure S1A in Supporting Information [SI]). Similar results were obtained for purified proteins at 1 μM each (data not shown). Interaction-dependent lipoylation could also be performed in living COS-7 cells, followed by cell lysis and immunoblot analysis, with a signal-to-background ratio of 15:1 (Figure 2). Furthermore, replacing the high-K_m LAP1 with the low-K_m substrates LAP2 and E2p produced high background labeling in the absence of an interaction inside COS-7 cells (Figure 2), as expected, validating our methodology design.

While gel-based analysis of interaction-dependent lipoylation in cells worked well, immunofluorescence detection after cell fixation was poor, due to background signal from endogenous lipoylated proteins in mitochondria. We only observed interaction-dependent lipoylation signal above mitochondrial background when FRB-LplA and FKBP-LAP1 were both strongly overexpressed (Figure S1B). We conclude from these studies that LplA and LAP1 suffice as the halves of an enzymatic complementation assay for PPI detection.

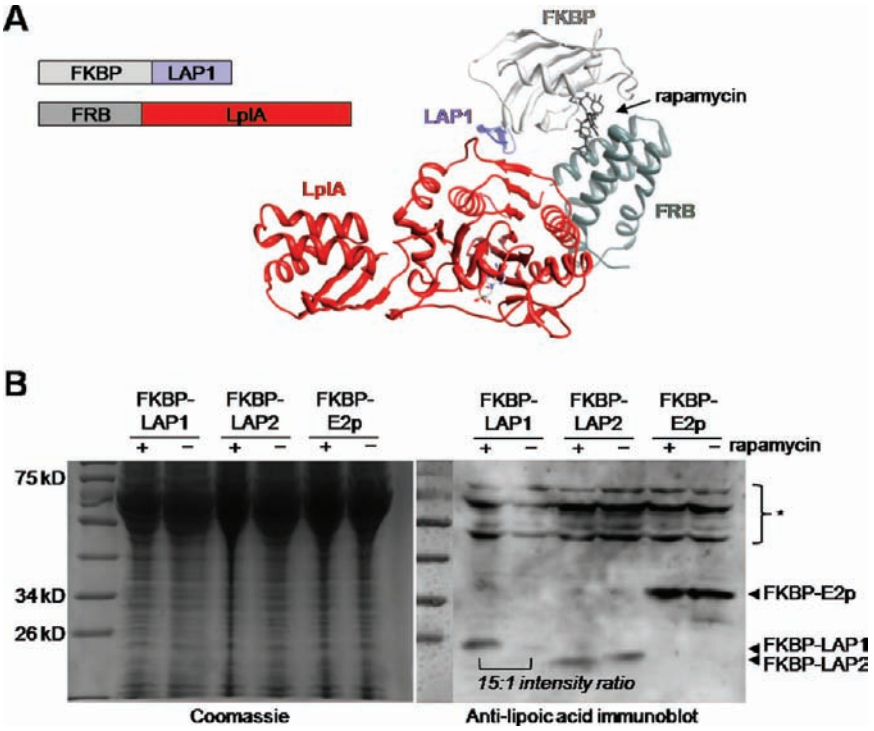

Figure 2. ID-PRIME reporter design and validation with lipoic acid. (A) Model of ternary complex of FRB-LplA, rapamycin, and FKBP-LAP1. Domain structures of constructs are shown to the left. Model was generated from PDB files 1FAP, 3A7R, and 1QJO. (B) COS-7 cells coexpressing FRB-LplA and FKBP-LAP1 were labeled with 500 μM lipoic acid for 1 min, with or without rapamycin pretreatment for 1 h. Cells were lysed, and lipoylated LAP1 was detected by anti-lipoic acid immunoblot. For comparison, FKBP-LAP1 was replaced with FKBP-LAP2 or FKBP-E2p. The starred bracket on the right indicates endogenous lipoylated mammalian proteins and possibly self-lipoylated FRB-LplA.

Interaction-Dependent Coumarin Ligation with Imaging Readout in Living Cells. While interaction-dependent lipoylation validated the use of LplA and LAP1 for a PPI reporter, lipoic acid detection requires antibody staining, so to develop our live-cell sensor, we replaced wild-type LplA with the coumarin ligase LplA^{W37V}. To perform labeling, FKBP-LAP1 and FRB-LplA^{W37V} are coexpressed in living cells. Addition of rapamycin promotes complex formation; treatment of cells with coumarin-AM$_2$ probe[11] (coumarin neutralized with two acetoxymethyl protecting groups) for 10 min allows coumarin loading into cells; subsequent incubation of cells in probe-free media for 30−60 min (as necessary, until maximal signal-to-background ratio is achieved) allows excess, unligated coumarin to leave the cell via organic anion transporters.

Performing ID-PRIME in living HEK cells produced coumarin labeling in transfected cells, but not neighboring untransfected cells (Figure 3). Background was undetectable in the absence of rapamycin. We note, however, with longer coumarin treatment times of >20 min, background coumarin signal began to accumulate in cells highly overexpressing the FKBP and FRB reporters (data not shown). The signal-to-background ratio for 10-min labeling was reproducibly >5:1 across experiments and sometimes as high as 15:1. Replacing the high-K_m LAP1 with the low-K_m substrate LAP2 produced high labeling in the absence of an interaction, as expected, again validating our reporter design.

Additional controls show that coumarin ID-PRIME is site-specific and enzyme-dependent (Figure 3). Mutating the lysine of LAP1 to alanine eliminated labeling, demonstrating that this is the unique site of coumarin attachment. Utilizing wild-type LplA, which has no coumarin ligation activity, in place of LplA^{W37V} also eliminated labeling. When the cells were fixed after coumarin labeling and washout (Figure S2, SI), immunofluorescence staining revealed that the coumarin-labeling pattern matched the localization of FKBP-LAP.

Characterization of ID-PRIME Method. Multiple mutants of LplA exhibit coumarin ligase activity.[11] The W37V mutation provides the highest sensitivity but exhibits increased background at high expression levels, compared to LplA^{W37I}.[11] We therefore compared ID-PRIME labeling of FKBP-LAP1 with FRB fusions to either LplA^{W37I} or LplA^{W37V} (Figure S3, SI). We observed better coumarin signal at low FKBP-LAP1 expression levels with FRB-LplA^{W37V}. However, background for LplA^{W37V} increased with expression level, while LplA^{W37I} background remained undetectable across all expression levels. Therefore, we recommend that the enzyme used for ID-PRIME labeling should be selected according to the system under study: proteins expressed at low levels may require LplA^{W37V} for optimal sensitivity, while LplA^{W37I} is preferable for highly over-expressed proteins, in order to maintain low background.

We investigated the generality of coumarin ID-PRIME in other cell lines and subcellular compartments (Figure S4, SI). ID-PRIME gave consistently high signal-to-background ratios for the FRB−FKBP system in HEK (Figure 3), COS7, and HeLa (Figure S4A, SI). ID-PRIME also reports the subcellular localization of PPIs. When the same experiment is performed, but FKBP constructs are restricted to the nucleus by appending a nuclear localization signal (NLS), the coumarin signal is also nuclear (Figure S4B, SI).

To test the tolerance of ID-PRIME for different fusion geometries, we compared our original constructs, FRB-LplA^{W37V} and FKBP-LAP1, to a swapped pair, FRB-LAP1 and

dx.doi.org/10.1021/ja206435e |J. Am. Chem. Soc. 2011, 133, 19769–19776

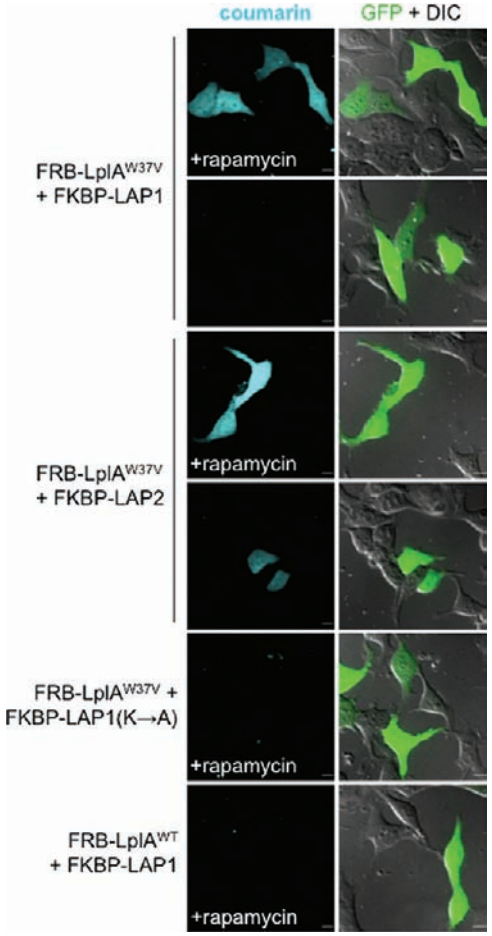

Figure 3. Imaging the FRB-FKBP interaction in living cells by ID-PRIME. HEK cells coexpressing FRB-LplA^{W37V} and FKBP-LAP1 were labeled with coumarin-AM$_2$ probe for 10 min, without or with rapamycin pretreatment for 1 h, to induce FRB-FKBP complexation. In the confocal images, GFP is a transfection marker. In the third and fourth rows, the same experiment was performed with FKBP-LAP2 (LAP2 is the high affinity peptide substrate for LplA) instead of FKBP-LAP1. Negative controls are shown with an alanine mutation in LAP1 (fifth row) and wild-type LplA in place of LplA^{W37V} (sixth row). Scale bars, 10 μm.

FKBP-LplA^{W37V} (Figure S5, SI). Both pairs exhibited low background in the absence of rapamycin, but not all of the cells transfected with the latter pair were stained with coumarin, in contrast to cells expressing the former reporter pair (data not shown). The FRB-LAP1−FKBP-LplA^{W37V} pair may have reduced sensitivity due to decreased ligase−peptide steric access. Therefore, when applying ID-PRIME to image new PPIs, it is important to make and test multiple LplA^{W37V} and LAP1 fusions to the proteins of interest.

We utilized an HPLC assay to measure the Michaelis−Menten parameters for ligation of coumarin probe to purified FKBP-LAP1 by LplA^{W37V} (Figure S6, SI). We were unable to provide a sufficiently high concentration of FKBP-LAP1 to saturate the initial reaction rate, so our data provide lower bounds for the Michaelis-Menten parameters. We measured a $k_{cat} > 0.45$ min^{-1}; while this catalytic rate is 22 times slower than lipoic acid ligation,[12] we estimate that it should be sufficient to label PPIs with a half life of ~1 minute or more. The K_m of the enzyme for LAP1 is greater than ~500 μM, providing an upper bound to protein concentrations that should be possible to study using ID-PRIME.

We also characterized the sensitivity of ID-PRIME by quantifying the coumarin labeling yield. We fused the red fluorescent protein mCherry to FKBP-LAP1, allowing us to quantify the concentration of this protein inside cells by comparison to a purified reference standard (the "wedge method" described in Supporting Methods).[14] We similarly quantified the concentration of ligated coumarin in live cells. The labeling yield was determined by plotting the coumarin concentration against the mCherry-FKBP-LAP1 concentration for single cells (Figure S7, SI). In the presence of rapamycin, a 10-min coumarin labeling gives a yield of 7.7 ± 0.6%. A similar labeling yield is observed after a 20-min coumarin labeling, suggesting that the FKBP−rapamycin−FRB complex does not turn over during this labeling time. By comparing the slopes of the +/− rapamycin linear fits (in Figure S7, SI), we determined that a minimum concentration of 6 μM mCherry-FKBP-LAP1 is required to give a signal-to-background ratio >2:1.

We wanted to determine if fusion of target proteins to LplA^{W37V} and LAP1 perturbs their interaction. To do this, we measured the apparent dissociation constant of FRB-LplA^{W37V} and FKBP-LAP1 by performing a rapamycin dose−response experiment. Because, as noted above, the FKBP−rapamycin−FRB complex probably does not dissociate during our labeling time, the single enzymatic turnover we detect provides a direct readout of the subpopulation of interacting proteins (though we note that, for a labile PPI, this will not be the case and a dissociation constant cannot be directly determined). We performed ID-PRIME labeling in cells treated with varying concentrations of rapamycin, and plotted the coumarin labeling intensity in single cells, measured by imaging, against rapamycin concentration (Figure 4). The dose−response curve thus generated can be fit with a dissociation constant of 3.1 ± 0.6 nM, in good agreement with the previously published K_d of 2.5 nM.[15] Therefore the interaction of FRB and FKBP does not appear to be perturbed by genetic fusion to the reporters.

Comparison of ID-PRIME to Bimolecular Fluorescence Complementation (BiFC). We wished to compare ID-PRIME to a well-characterized imaging-based PPI reporter. Bimolecular fluorescence complementation (BiFC) has been applied to the visualization of hundreds of PPIs inside living mammalian cells due to its ease of use, good sensitivity, and low background.[2] In BiFC, enhanced yellow fluorescent protein (YFP) is split into two nonfluorescent fragments, which, when fused to interacting proteins, associate and fold to reconstitute YFP.[16] To quantitatively compare ID-PRIME to BiFC, we fused the BiFC reporter fragments YN155 and YC155[16] to the C-terminal ends of FRB and FKBP, respectively, to make them as similar to our ID-PRIME constructs as possible. We then expressed the BiFC reporters in HEK cells in the presence or absence of rapamycin at a normal growth temperature of 37 °C, or at the reduced temperature of 30 °C, which reportedly increases BiFC signal by promoting YFP fluorophore maturation.[17] ID-PRIME reporter-expressing cells were grown and labeled under identical conditions to facilitate direct comparison between the methods. We then fixed the cells to assay expression of all constructs by immunostaining prior to YFP and coumarin imaging. Linear regression analysis of the single-cell plots revealed that, while the absolute signal for BiFC was about twice as high for cells grown at 30 °C relative to cells grown at 37 °C, the signal-to-background ratio was approximately 8:1 for both conditions (Figure S8, SI),

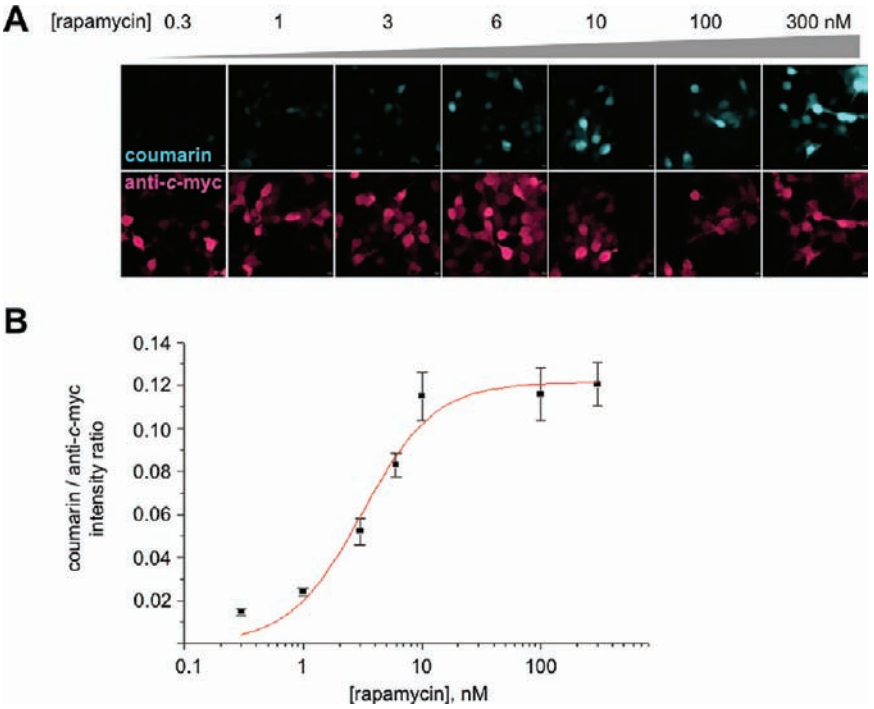

Figure 4. Rapamycin dose−response curve. (A) HEK cells coexpressing FKBP-LAP1 and FRB-LplA^{W37V} were incubated with varying concentrations of rapamycin for 1 h, then labeled with coumarin-AM_2 for 10 min. After fixation, total FKBP-LAP1 was detected with anti-*c*-myc antibody. (B) The graph shows the mean coumarin/anti-*c*-myc intensity ratio for 8−25 cells from at least three fields of view for each rapamycin condition. Error bars, ± standard error of the mean (sem); scale bars, 10 μm.

similar to the 10:1 ratio previously reported for BiFC.[1] In analogous experiments, the ID-PRIME signal-to-background ratio ranged from 5:1 to 15:1. We conclude that, ID-PRIME provides a similar signal-to-background response as BiFC while addressing the limitations of temporal resolution and complex trapping.

Application of ID-PRIME to Imaging of Other Protein-Protein Interactions. To test the generality of ID-PRIME, we applied the method to the imaging of another cellular PPI, the interaction between the leucine zipper domains of the transcription factors Fos and Jun. These domains specifically heterodimerize to form a parallel coiled coil.[18,19] LplA^{W37V} was fused to the C-terminus of the Jun fragment, and LAP1 was fused to the C-terminus of the Fos fragment. To serve as a negative control, we also prepared the ΔZIP mutant of Fos-LAP1, with the leucine zipper-forming residues deleted.[20] These constructs are similar to those originally used to validate the BiFC methodology,[20] but lack the N-terminal nuclear targeting sequence and are therefore cytoplasmically localized. Applying the standard ID-PRIME-labeling protocol to HEK cells produced coumarin signal in transfected cells (Figure 5A, top row). Negative controls with LplA^{W37V}, alone (not fused to Jun), or with Fos(ΔZIP)-LAP1, gave ∼4-fold lower signal (Figures 5A and 5B), although coumarin labeling was still detectable above background, suggesting some non-specificity due to over-expression of the Fos and Jun constructs.

We also applied ID-PRIME to the visualization of a challenging PPI, the interaction of neuroligin-1 with PSD-95. Neuroligin-1 is a postsynaptic adhesion protein that interacts with presynaptic neurexins across the synaptic cleft to promote excitatory synapse formation and maturation.[21−23] The intracellular interaction of the C terminus of neuroligin-1 with the third PDZ domain of PSD-95,[24] a postsynaptic scaffolding protein, has been implicated in this process.[25] The membrane localization of this interacting pair, as well as the sensitivity of the interaction to genetic fusions of neuroligin at the C terminus,[26] makes it challenging to detect.

We demonstrated that ID-PRIME can specifically label the interaction of PSD-95 and neuroligin-1 in HEK cells. We fused LAP1 to the intracellular portion of neuroligin-1, at the T776 site previously shown to tolerate insertions without perturbing the localization of the protein.[26] We fused LplA^{W37V} to the C-terminus of PSD-95, the same location previously reported for fluorescent protein fusions.[27,28] When these constructs are coexpressed in living HEK cells, our coumarin labeling protocol affords membrane-localized neuroligin-1-LAP1 labeling (Figure 5C, top row). As a negative control, we prepared neuroligin-1(ΔPDZ)-LAP1, deleting the three C-terminal amino acids of neuroligin-1-LAP1 to abolish interaction with PSD-95.[24] Coexpression of neuroligin-1(ΔPDZ)-LAP1 with PSD-95-LplA^{W37V} eliminated coumarin labeling (Figure 5C, second row). Similarly, coexpressing neuroligin-1-LAP1 with LplA^{W37V} in the absence of fusion to PSD-95 afforded no coumarin labeling (Figure 5C, bottom row). We can therefore specifically label this interaction in heterologous cells.

In conclusion, we have developed ID-PRIME for imaging PPIs in living cells. With a total labeling time of 40−60 min, ID-PRIME visualizes interactions of proteins expressed at micromolar concentrations inside living cells. While the total labeling time is at least 40 min, we note that only interactions that occur during the 10-min coumarin incubation are visualized. ID-PRIME is complementary to the well-established BiFC method, in that it utilizes a short labeling protocol and does not trap interacting proteins in complex. This method also represents an improvement over our previous interaction-dependent

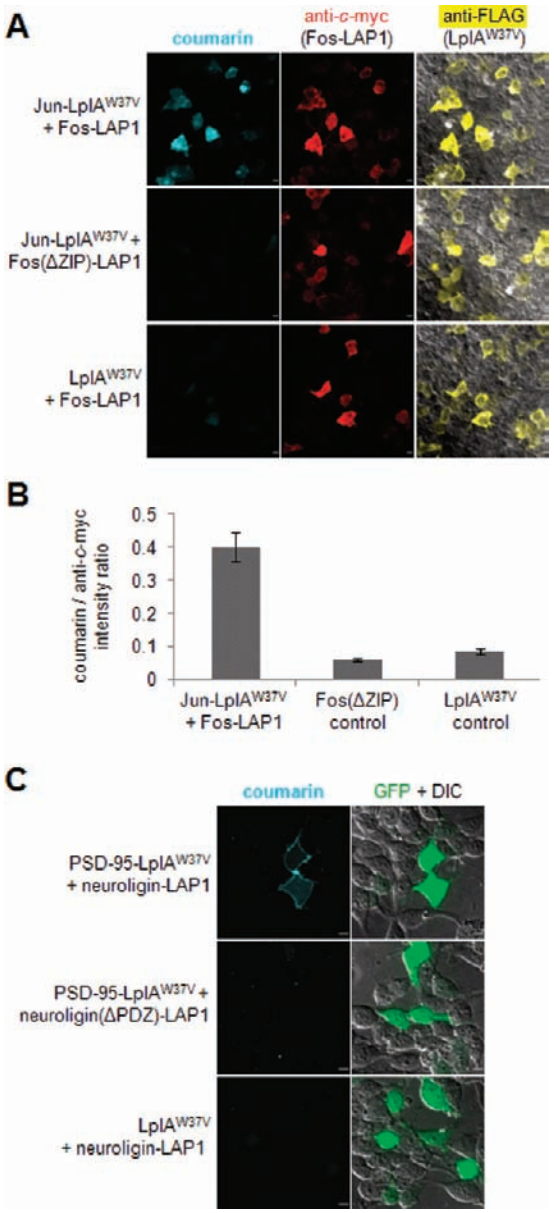

Figure 5. ID-PRIME for imaging the interaction between Fos and Jun, and neuroligin-1 and PSD-95. (A) Imaging the interaction of Fos and Jun in HEK cells. HEK cells coexpressing Jun-LplA^{W37V} and Fos-LAP1 were labeled with coumarin-AM_2 for 5 min, then washed for 30 min, fixed and immunostained prior to imaging as described in the Methods. Anti-*c*-myc visualizes Fos, and anti-FLAG visualizes Jun/LplA. Negative controls are shown with FosΔZIP-LAP1, an interaction-deficient deletion mutant of Fos, and LplA^{W37V} in place of Jun-LplA^{W37V}. Scale bars, 10 μm. (B) Quantitative analysis of Fos—Jun labeling. The graph shows the mean coumarin/anti-*c*-myc intensity ratio averaged for 24 cells from each condition (error bars ± sem). (C) Imaging the interaction of PSD-95 and neuroligin-1 in HEK cells. HEK cells coexpressing PSD-95-LplA^{W37V} and AP-neuroligin-1-LAP1 were labeled with coumarin-AM_2 for 10 min, then washed for 60 min prior to live imaging. GFP is a transfection marker. Negative controls are shown with AP-neuroligin-1(ΔPDZ)-LAP1, an interaction-deficient mutant of neuroligin-1, and LplA^{W37V} in place of PSD-95-LplA^{W37V}. Scale bars, 10 μm.

biotinylation method for PPI imaging,[6] because it is compatible with the interior of living cells, and detection requires only one, rather than two (biotin followed by streptavidin), labeling steps.

We have not experimentally tested the limits of K_d and half-life of PPIs that can be detected by this method. We note that the k_{cat} of LplA^{W37V} for LAP1 is expected to be the primary determinant of sensitivity, and, as stated above, will probably limit application of the method to PPIs with a half-life greater than 1 min. Transient PPI detection will require the development of faster fluorophore ligases.

In future work, we hope to engineer the catalytic properties of LplA to improve the utility of ID-PRIME, in particular by extending LplA labeling to the cell surface and secretory pathway, by incorporating red-shifted fluorophores with emission farther from cellular autofluorescence, and by improving ligation kinetics to improve detection of transient PPIs. Another goal is to develop dynamic reporters that respond to both increases and decreases in PPIs in real time, which is currently not possible with either ID-PRIME or BiFC.

METHODS

Cloning and Mutagenesis. Nucleotide sequences of all constructs are available at http://stellar.mit.edu/S/project/tinglabreagents/r02/materials.html. Constructs were prepared by standard restriction cloning methods or QuikChange mutagenesis (Stratagene).

Peptide Sequences. While our previous reports[9,10] recommended 22-amino acid sequences for LAP1 (DEVLVEIETDKAVLEVPGGEEE or DEVLVEIETDKAVLEVPASADG) we determined in this study that, for the purposes of interaction-dependent labeling, the originally designed 17-amino acid LAP1 sequence[9] (DEVLVEIETDKAVLEVP) is coumarin-labeled with equivalent efficiency to the 22-mer (data not shown). Therefore all constructs utilize the 17-mer LAP1 peptide.

Mammalian Cell Culture. HEK, HeLa, and COS-7 cells were cultured in growth media consisting of Dulbecco's modification of Eagle's medium (DMEM, Cellgro) supplemented with 10% fetal bovine serum (FBS, PAA Laboratories), 50 units/mL penicillin, and 50 μg/mL streptomycin (Cellgro). Cells were maintained at 37 °C under an atmosphere of 5% CO_2 unless otherwise noted. For imaging, cells were grown on glass coverslips. HeLa and COS-7 cells were grown directly on glass. HEK cells were grown on glass pretreated with 50 μg/mL fibronectin (Millipore).

Fluorescence Imaging. Cells were imaged in Dulbecco's phosphate-buffered saline (DPBS) on glass coverslips. A Zeiss Axiovert 200 M inverted microscope with a 40× oil-immersion objective was used for epifluorescence imaging. Coumarin (400/20 excitation, 425 dichroic, 435/30 emission), YFP/Alexa Fluor 488 (493/16 excitation, 506 dichroic, 525/30 emission), mCherry/Alexa Fluor 568 (570/20 excitation, 585 dichroic, 605/30 emission), Alexa Fluor 647 (630/20 excitation, 660 dichroic, 680/30 emission), and differential interference contrast (DIC) images were collected using Slidebook 5.0 (Intelligent Imaging Innovations). Confocal imaging was performed with a Zeiss AxioObserver inverted microscope with 40 × and 63 × oil-immersion objectives, outfitted with a Yokogawa spinning disk confocal head, a Quad-band notch dichroic mirror (405/488/568/647), and 405 (diode), 491 (DPSS), 561 (DPSS), and 640 nm (diode) lasers (all 50 mW). Coumarin (405 laser excitation, 445/40 emission), GFP/Alexa Fluor 488 (491 laser excitation, 528/38 emission), Alexa Fluor 568 (561 laser excitation, 617/73 emission), Alexa Fluor 647 (640 laser excitation, 700/75 emission), and DIC images were collected using Slidebook. All image analysis was performed in SlideBook . Fluorophore channels in each experiment were normalized to the same intensity ranges. Acquisition times ranged from 20 ms to 5 s. Images were confocal except where indicated.

Immunoblot Detection of Interaction-Dependent Lipoylation in Cells (Figure 2). COS-7 cells were grown to 50%

confluency in a 24-well plate, then transfected with 600 ng of FRB-LplA-pcDNA3 and 600 ng of FKBP-LAP1-pcDNA3 per well using Lipofectamine 2000 (Invitrogen) according to the manufacturer's instructions. For comparison, FKBP-LAP1-pcDNA3 was replaced with FKBP-LAP2-pcDNA3 or FKBP-E2p-pcDNA3 in control samples. Twenty-four hours after transfection, growth media was removed, and fresh growth media containing 100 nM rapamycin was applied to the cells for one hour at 37 °C. Rapamycin was omitted from parallel wells as a negative control. The media was then removed, and prewarmed DPBS containing 500 μM lipoic acid was applied to the cells for one minute. We found that increasing the lipoic acid labeling time to three minutes increased the background (and decreased the signal-to-noise ratio to 2.5:1) (data not shown); therefore restricting the labeling to one minute is crucial. After labeling, the lipoic acid solution was removed and cells were immediately lysed (and the reaction quenched) with direct application of SDS-PAGE loading buffer (40 μL per well). Samples were denatured by boiling for 5 min. Thirty microliters of this material was loaded into each well of a 14% acrylamide SDS-PAGE gel.

For Western blotting, proteins were transferred from gels to nitrocellulose for 120 min at 500 mA. (Identical parallel reactions were run on an SDS-PAGE gel, then stained with Coommassie brilliant blue, as a loading control.) After transfer, membranes were blocked with 3% bovine serum albumin (BSA) in Tris-buffered saline with 0.05% Tween-20 (TBS-T) for 1 h at room temperature. For lipoic acid detection, the membrane was treated with rabbit polyclonal anti-lipoic acid antibody (Calbiochem) at a 1:300 dilution in 3% BSA in TBS-T at room temperature for one hour, then washed three times for 5 min with TBS-T. The membrane was then incubated with goat anti-rabbit horseradish peroxidase conjugate (Bio-Rad) in 3% BSA in TBS-T at a 1:3000 dilution for one hour at room temperature, then again washed three times for 5 min with TBS-T. Chemiluminescence detection was performed with SuperSignal West Femto reagent (Pierce), and imaged on an Alpha Innotech ChemiImager 5500. Spot densitometry was performed using AlphaEase FC version 3.2.2 software (Alpha Innotech). A rectangle was drawn around the visible extent of each band, and an identical box was drawn on the background neighboring each band of interest. The background-subtracted intensity values were then ratioed to assess labeling signal-to-background.

Coumarin ID-PRIME in HEK Cells (Figure 3). HEK cells were grown to 70% confluency on fibronectin-coated glass coverslips, then transfected with 400 ng of FRB-LplA^{W37V}-pcDNA3, 400 ng of FKBP-LAP1-pcDNA3, and 20 ng of GFP as a cotransfection marker per 0.95 cm^2 using Neofectin (Mid-Atlantic Biolabs) according to the manufacturer's instructions. Twenty-four hours after transfection, 100 nM rapamycin was added in growth media for 1 h at 37 °C, or omitted as a negative control. Growth media was then removed, and the cells were labeled by applying 20 μM coumarin-AM$_2$ in serum-free DMEM at 37 °C for 10 min. Excess coumarin was washed out with three changes of fresh DMEM over 60 min at 37 °C. Cells were imaged in DPBS in confocal mode at 63× magnification. Negative control experiments were performed with the indicated construct substitutions.

Rapamycin Dose−Response (Figure 4). HEK cells were grown to 70% confluency on fibronectin-coated glass coverslips, then transfected with 400 ng of FRB-LplA^{W37V}-pcDNA3 and 400 ng of FKBP-LAP1-pcDNA3 per 0.95 cm^2 using Lipofectamine 2000 (Invitrogen) according to the manufacturer's instructions. Twenty-four hours after transfection, concentrations of rapamycin ranging from 0.3 to 300 nM were added in growth media for 1 h at 37 °C. Growth media was then removed, and the cells were labeled by applying 20 μM coumarin-AM$_2$ in serum-free DMEM at 37 °C for 10 min. Excess coumarin was washed out with one application of fresh DMEM for 30 min. Cells were then fixed with 3.7% paraformaldehyde in DPBS at 4 °C for 10 min, and then permeabilized with cold methanol at −20 °C for 10 min. Fixed cells were washed with DPBS, then blocked overnight in blocking buffer (3% BSA in DPBS with 0.1% Tween-20, or DPBS-T) at 4 °C. Cells were then immunostained serially with 1:1000 dilutions in blocking buffer of the following antibodies in the following order: for one hour each at room temperature: mouse anti-*c*-myc, goat anti-mouse Alexa Fluor 647 conjugate, rabbit anti-HA, goat anti-rabbit Alexa Fluor 568 conjugate. Three 5-min DPBS washes were applied between each antibody incubation step. Epifluorescence images of cells in DPBS were acquired at 40× magnification.

For quantitation, regions of interest (ROIs) were manually drawn on transfected cells by visually inspecting the anti-*c*-myc immunofluorescence images. Average intensities of coumarin, anti-*c*-myc immunofluorescence, and anti-HA immunofluorescence were computed. Background correction was applied by drawing a ROI on an untransfected cell in each field of view and subtracting these background intensities from all values generated from that particular field of view. ROIs with anti-HA intensities greater than 3000 were kept for analysis, leaving at least eight data points for each rapamycin concentration and as many as 25. The coumarin intensity was ratioed to the anti-*c*-myc intensity for each ROI; these values were averaged for each rapamycin concentration.

Coumarin ID-PRIME to Detect the Interaction of Fos and Jun (Figure 5). HEK cells were grown to 80% confluency on fibronectin-coated glass coverslips, then transfected with 50 ng of Jun-LplA^{W37V}-pcDNA3 and 400 ng of Fos-LAP1-pcDNA3 per 0.95 cm^2 using Lipofectamine 2000 (Invitrogen) according to the manufacturer's instructions. Negative controls were performed by substituting the Fos construct with 400 ng of Fos(ΔZIP)-LAP1-pcDNA3 or by substituting the Jun construct with 50 ng of FLAG-LplA^{W37V}. Twenty-four hours after transfection, the cells were labeled by applying 20 μM coumarin-AM$_2$ in serum-free DMEM at 37 °C for 5 min. Excess coumarin was washed out with three changes of fresh DMEM over 30 min at 37 °C. Cells were then fixed with 3.7% paraformaldehyde in DPBS at room temperature for 15 min, then permeabilized with cold methanol at −20 °C for 10 min. Fixed cells were washed with DPBS, then blocked for 3 h in blocking buffer at room temperature. Cells were then immunostained serially with 1:1000 dilutions in blocking buffer of the following antibodies in the following order, for 20 min each at room temperature: mouse anti-FLAG, goat anti-mouse Alexa Fluor 488 conjugate, chicken anti-*c*-myc, goat anti-chicken Alexa Fluor 568 conjugate. Three rinses with DPBS with 0.1% Tween-20 was applied between each antibody incubation step. Confocal images were acquired at 40× magnification.

To quantify interaction-dependent coumarin labeling, ROIs were manually drawn on transfected cells by visually inspecting the anti-*c*-myc immunofluorescence images. Average intensities of coumarin, anti-*c*-myc immunofluorescence, and anti-FLAG immunofluorescence were computed. Background fluorescence was measured by drawing a ROI on an untransfected cell in each of nine fields of view.

Coumarin ID-PRIME to Detect the Interaction of PSD-95 and Neuroligin-1 (Figure 5). HEK cells were grown to 70% confluency on fibronectin-coated glass coverslips, then transfected with 100 ng of PSD-95-LplA^{W37V}-pNICE, 500 ng of AP-neuroligin-1-LAP1-pNICE, and 20 ng of GFP per cm^2 using Neofectin according to the manufacturer's instructions. For negative controls, AP-neuroligin-1-LAP1-pNICE was replaced with an equal amount of AP-neuroligin-1(ΔPDZ)-LAP1-pNICE, or PSD-95-LplA^{W37V}-pNICE was replaced with 20 ng of FLAG-LplA^{W37V}-pcDNA3 (due to overexpression). Twenty-four hours after transfection, the cells were labeled by applying 20 μM coumarin-AM$_2$ in serum-free DMEM at 37 °C for 10 min. Excess coumarin was washed out with three changes of fresh DMEM over 60 min at 37 °C. Cells were imaged in DPBS in confocal mode with 63× magnification.

■ ASSOCIATED CONTENT

Supporting Information. Supporting Figures 1−8 (interaction-dependent lipoylation in vitro and in cells, comparison of

coumarin ligase mutants, ID-PRIME in other cell lines and the nucleus, alternate fusion geometries, labeling yield and sensitivity analysis, kinetics of coumarin ligation, and comparison of ID-PRIME and BiFC), and supporting methods. This material is available free of charge via the Internet at http://pubs.acs.org.

AUTHOR INFORMATION

Corresponding Author
ating@mit.edu

Present Addresses
[‡]Department of Chemistry and Chemical Biology, Harvard University, Cambridge, MA 02138

ACKNOWLEDGMENT

We thank Chayasith Uttamapinant, Katharine White, Marta Fernández-Suárez, Jeffrey Martell, and Ken Loh for reagents and helpful advice; Joshua Sanes and Masahito Yamagata for the PSD-95 expression plasmid; Tom Kerppola for YFP BiFC genes; and Amy Keating for Fos and Jun genes. This work was supported by the National Institutes of Health (R01 GM0726 70), the Dreyfus Foundation, a Genentech/American Chemical Society Organic Division predoctoral fellowship and a David A. Johnson summer fellowship (to S.A.S.).

REFERENCES

(1) Robida, A. M.; Kerppola, T. K. *J. Mol. Biol.* **2009**, *394*, 391.
(2) Kerppola, T. K. *Nat. Rev. Mol. Cell Biol.* **2006**, *7*, 449.
(3) Zamyatnin, A. A., Jr.; Solovyev, A. G.; Bozhkov, P. V.; Valkonen, J. P.; Morozov, S. Y.; Savenkov, E. I. *Plant J.* **2006**, *46*, 145.
(4) Tilsner, J.; Cowan, G. H.; Roberts, A. G.; Chapman, S. N.; Ziegler, A.; Savenkov, E.; Torrance, L. *Virology* **2010**, *402*, 41.
(5) Walter, M.; Chaban, C.; Schutze, K.; Batistic, O.; Weckermann, K.; Nake, C.; Blazevic, D.; Grefen, C.; Schumacher, K.; Oecking, C.; Harter, K.; Kudla, J. *Plant J.* **2004**, *40*, 428.
(6) Fernandez-Suarez, M.; Chen, T. S.; Ting, A. Y. *J. Am. Chem. Soc.* **2008**, *130*, 9251.
(7) Beckett, D.; Kovaleva, E.; Schatz, P. J. *Protein Sci.* **1999**, *8*, 921.
(8) Chen, I.; Howarth, M.; Lin, W.; Ting, A. Y. *Nat. Methods* **2005**, *2*, 99.
(9) Fernandez-Suarez, M.; Baruah, H.; Martinez-Hernandez, L.; Xie, K. T.; Baskin, J. M.; Bertozzi, C. R.; Ting, A. Y. *Nat. Biotechnol.* **2007**, *25*, 1483.
(10) Baruah, H.; Puthenveetil, S.; Choi, Y. A.; Shah, S.; Ting, A. Y. *Angew. Chem., Int. Ed.* **2008**, *47*, 7018.
(11) Uttamapinant, C.; White, K. A.; Baruah, H.; Thompson, S.; Fernandez-Suarez, M.; Puthenveetil, S.; Ting, A. Y. *Proc. Natl. Acad. Sci. U.S.A.* **2010**, *107*, 10914.
(12) Puthenveetil, S.; Liu, D. S.; White, K. A.; Thompson, S.; Ting, A. Y. *J. Am. Chem. Soc.* **2009**, *131*, 16430.
(13) Choi, J.; Chen, J.; Schreiber, S. L.; Clardy, J. *Science* **1996**, *273*, 239.
(14) Adams, S. R.; Campbell, R. E.; Gross, L. A.; Martin, B. R.; Walkup, G. K.; Yao, Y.; Llopis, J.; Tsien, R. Y. *J. Am. Chem. Soc.* **2002**, *124*, 6063.
(15) Chen, J.; Zheng, X. F.; Brown, E. J.; Schreiber, S. L. *Proc. Natl. Acad. Sci. U.S.A.* **1995**, *92*, 4947.
(16) Hu, C. D.; Chinenov, Y.; Kerppola, T. K. *Mol. Cell* **2002**, *9*, 789.
(17) Kerppola, T. K. *Nat. Protoc.* **2006**, *1*, 1278.
(18) O'Shea, E. K.; Rutkowski, R.; Stafford, W. F., III; Kim, P. S. *Science* **1989**, *245*, 646.
(19) Reinke, A. W.; Grant, R. A.; Keating, A. E. *J. Am. Chem. Soc.* **2010**, *132*, 6025.
(20) Hu, C. D.; Chinenov, Y.; Kerppola, T. K. *Mol. Cells* **2002**, *9*, 789.
(21) Song, J. Y.; Ichtchenko, K.; Sudhof, T. C.; Brose, N. *Proc. Natl. Acad. Sci. U.S.A.* **1999**, *96*, 1100.
(22) Ichtchenko, K.; Hata, Y.; Nguyen, T.; Ullrich, B.; Missler, M.; Moomaw, C.; Sudhof, T. C. *Cell* **1995**, *81*, 435.
(23) Ichtchenko, K.; Nguyen, T.; Sudhof, T. C. *J. Biol. Chem.* **1996**, *271*, 2676.
(24) Irie, M.; Hata, Y.; Takeuchi, M.; Ichtchenko, K.; Toyoda, A.; Hirao, K.; Takai, Y.; Rosahl, T. W.; Sudhof, T. C. *Science* **1997**, *277*, 1511.
(25) Prange, O.; Wong, T. P.; Gerrow, K.; Wang, Y. T.; El-Husseini, A. *Proc. Natl. Acad. Sci. U.S.A.* **2004**, *101*, 13915.
(26) Sara, Y.; Biederer, T.; Atasoy, D.; Chubykin, A.; Mozhayeva, M. G.; Sudhof, T. C.; Kavalali, E. T. *J. Neurosci.* **2005**, *25*, 260.
(27) Heine, M.; Thoumine, O.; Mondin, M.; Tessier, B.; Giannone, G.; Choquet, D. *Proc. Natl. Acad. Sci. U.S.A.* **2008**, *105*, 20947.
(28) de Wit, J.; Sylwestrak, E.; O'Sullivan, M. L.; Otto, S.; Tiglio, K.; Savas, J. N.; Yates, J. R., III; Comoletti, D.; Taylor, P.; Ghosh, A. *Neuron* **2009**, *64*, 799.